The Effect of Additives on the Reaction of Portland and Alumina Cement Components with Water. Time Resolved Powder Neutron Diffraction Investigations

A. Nørlund Christensen[a]*, H. Fjellvåg[b] and M. S. Lehmann[b]

[a]Department of Inorganic Chemistry, Aarhus University, DK-8000 Aarhus C, Denmark. [b]Institut Max von Laue – Paul Langevin, F-38042 Grenoble Cedex, France

Christensen, A. Nørlund, Fjellvåg, H. and Lehmann, M. S., 1986. The Effect of Additives on the Reaction of Portland and Alumina Cement Components with Water. Time Resolved Powder Neutron Diffraction Investigations. – Acta Chem. Scand. A 40: 126–141.

The effect of additives on the reactions between D_2O and the cement clinker components $Ca_3Al_2O_6$, $Ca_{12}Al_{14}O_{33}$, and $CaAl_2O_4$ was investigated by on-line powder neutron diffraction at temperatures up to 120 °C. The additives used were $CaSO_4 \cdot \frac{1}{2}D_2O$, $CaSO_4 \cdot 2D_2O$, $CaCO_3$, $Ca(OD)_2$, $CaCl_2$, and SiO_2. For the sulphate containing systems a precursor phase was observed before the formation of ettringite was initiated. The precursor starts to disappear simultaneously with the onset of the formation of ettringite. With $CaCO_3$ as additive the final product was $Ca_4Al_2(OD)_{12}CO_3 \cdot 5D_2O$, while with $CaCl_2$ as additive the final product was β-$Ca_4Al_2O_6Cl_2 \cdot 10D_2O$. The compounds $Ca(OD)_2$ and SiO_2 had no significant effect on the rates of hydrolysis at the temperatures investigated.

Calcium aluminates and calcium silicates constitute the main components of cement clinker. The hydration properties of these phases were studied by means of time resolved powder neutron diffraction and discussed in Refs. 1,2. However, the hydration properties as measured by the reaction rates are dependent on parameters such as particle size and size distribution functions, solid/water ratios, temperature, the presence of additives, etc. This study is concerned with the effect of additives on the hydration reactions of calcium aluminates ($Ca_3Al_2O_6$, $Ca_{12}Al_{14}O_{33}$, and $CaAl_2O_4$, or C_3A, $C_{12}A_7$, and CA, according to common abbreviations in cement literature). The possibility of monitoring the setting properties of cement mortars by appropriate choice of mixing ratios with different additives makes this an important aspect of cement chemistry.

In the present study, $CaCO_3$, $Ca(OD)_2$, $CaSO_4 \cdot \frac{1}{2}D_2O$, $CaSO_4 \cdot 2D_2O$, $CaCl_2$, and SiO_2 were used as additives. In the abbreviated notation S means SiO_2, $\bar{C}$ CO_2, D D_2O, H H_2O, and $\bar{S}$ is SO_3, and the notations for phases here discussed are listed in Table 1. The hydration reactions were studied by means of on-line powder neutron diffraction which makes it possible to study the reactions in real time. An advantage of this method is the *in situ* identification and registration of amounts of crystalline phases (reactants and products). This is in contrast to methods where the events of the hydrolysis reactions are deduced indirectly from measurements of the properties of the end products, *e.g.* differential thermal analysis of set cement pastes.[3]

Experimental

The phases C_3A, $C_{12}A_7$, and CA were made from stoichiometric proportions of the oxides (CaO and Al_2O_3). $C_{12}A_7$ was made by zone melting while C_3A and CA were synthesized by sintering of powder mixtures in a crucible furnace at 1400 °C for three periods of 24 h, with intermediate crushing of the samples. The starting ma-

*To whom correspondence should be addressed.

Table 1. Chemical formulae and short-hand notation for some phases discussed in the text.

$Ca_3Al_2O_6$	C_3A	$Ca_3Al_6(OD)_{24} \cdot 18D_2O$	CAD_{10}
$Ca_{12}Al_{14}O_{33}$	$C_{12}A_7$	$Ca_6Al_2(OD)_{12}(SO_4)_3 \cdot 26D_2O$	$C_6A\bar{S}_3D_{32}$
$CaAl_2O_4$	CA	$Ca_4Al_2(OD)_{12}SO_4 \cdot 6D_2O$	$C_4A\bar{S}D_{12}$
$Ca_3Al_2(OD)_{12}$	C_3AD_6	$Ca_4Al_2(OD)_{12}CO_3 \cdot 5D_2O$	$C_4A\bar{C}D_{11}$
$2CaO \cdot Al_2O_3 \cdot 6D_2O$	C_2AD_6	$Ca_2Al(OD)_7 \cdot 3D_2O$	C_4AD_{13}
$Ca_2Al(OD)_{10} \cdot 3D_2O$	C_2AD_8	$Ca_2Al(OD)_7 \cdot 6D_2O$	C_4AD_{19}

terials were Al_2O_3 and $CaCO_3$ (Merck, analytical grade). CaO was made by heating $CaCO_3$ at 1000 °C for 8 h.

$CaSO_4 \cdot \frac{1}{2}D_2O$ was made by first dehydrating $CaSO_4 \cdot 2H_2O$ (Merck, analytical grade) at 150 °C and then allowing the product to react with D_2O at room temperature. This treatment was repeated 3 times.[4] The formula $CaSO_4 \cdot \frac{1}{2}D_2O$ is here adopted for phases belonging to the group of hemihydrates (or as here, their deuterated forms) with variable amounts of crystal bound water (*viz.* 0.50, 0.67, 0.8 D_2O *etc.*). The recorded neutron diffraction powder pattern of the present $CaSO_4 \cdot \frac{1}{2}D_2O$ sample corresponded well to that calculated on the basis of the structure of $CaSO_4 \cdot 0.67\ D_2O$[5] (D-atoms not considered). $Ca(OD)_2$ was made by reaction of CaO with D_2O. The other substances used were $CaCl_2$ (Merck, min. 95 % $CaCl_2$) and SiO_2 (Prolabo). All powders used in the neutron diffraction experiments were selected from the fraction that could pass a 150 mesh (~0.11 mm) sieve.

The purity of the starting materials was checked by Guinier photographs ($CuK\alpha_1$ radiation, Si as internal standard). The C_3A samples contained a minor impurity of $C_{12}A_7$. However, this is believed not to influence the hydration properties significantly.[6]

Powder neutron diffraction data were recorded with the D1B diffractometer situated at the ILL, Grenoble, $\lambda = 2.517$ Å. A 400 cell multidetector covered a 2θ range of 80°. In a typical experiment, 3.00 g solid substance was mixed with 3.75 ml D_2O (99.7 %) in an 11 mm diameter vanadium sample holder. The water to solid ratio was 1.27 by weight, which is somewhat larger than usually applied in investigations of cement mortars (ratios of 0.3–1.0). The temperature could be controlled within ±1 °C and varied between 25 and 150 °C. The mixing ratios between calcium aluminates and additives in the experiments are given in Table 2. Recorded intensities were extracted at 5, 10, or 20 min intervals, depending on the actual reaction rate (*cf.* Refs. 1,2 for further details).

Integrated intensities of Bragg reflections were evaluated by the programme INTEGRE[7] and normalized to a standard monitor count. The integrated intensities are, in the absence of absorption or preferred orientation effects, proportional to the amount of sample, and hence useful for measuring the hydration rates of crystalline phases. Calculated diffraction patterns were for purpose of phase identification, obtained by the LAZY-PULVERIX programme.[8] The programme input requires knowledge of the atomic positions in the unit cell. However, in the case of neutron diffraction this implies that H/D positions must also be known (due to their significant scattering contributions). Unfortunately, this is not the case for many complex hydrates and the identification process is therefore more difficult.

Since the structure factor calculations are based on the positions of all atoms in the unit cell, quantitative comparisons of different phases can be made from integrated intensities of Bragg reflections ascribed to the various phases. A scale factor relating observed and calculated intensities was deduced from calibration runs of weighed amounts of $CaSO_4 \cdot 2D_2O$. However, the factor is sensitive to variations in the sample positioning relative to the neutron beam, and not all experiments could be analysed according to this procedure.

The integrated intensity of the broad water (liquid) peak in the diffraction pattern is similarly related to the amount of D_2O present. Any contribution to this peak from amorphous phases was assumed to be negligible. The variation of free water was estimated by comparing integrated intensities over 2° (in 2θ) on the low-angle side of the peak maximum.

Table 2. Phases identified in the powder neutron and X-ray diffraction diagrams. F: in first diagram; L: in last diagram; I: intermediate phase; X: after 80 d (X-ray). Molar ratio is mmol of formula units of calcium aluminate/ mmol formula units of additive. The quantities in mmol add up to the mass 3.0 g of solid mixture, and to this quantity 3.75 ml D_2O was used in the reactions.

Table 2a.

Sample mixture	Ratios (mmols)	T (°C)	Total time (h)	β-$CaSO_4$	$CaSO_4 \cdot \frac{1}{2}D_2O$	$CaSO_4 \cdot 2D_2O$	Monosulphate	Ettringite	Precursor	$Ca(OD)_2$	C_3AD_6	α-C_4AD_{19}
$C_3A + CaSO_4 \cdot \frac{1}{2}D_2O$	4.26/12.85	60	3.0		F	L			L			
$C_3A + CaSO_4 \cdot 2D_2O$	3.78/11.38	60	3.0			FL			L			
$C_3A + CaSO_4 \cdot \frac{1}{2}D_2O$	4.26/12.85	115	2.0	L	FL							
$C_3A + CaSO_4 \cdot 2D_2O$	10.00/ 1.72	27	10.5				X	L	I		X	
$C_3A + CaSO_4 \cdot 2D_2O$	10.00/ 1.72	50	11.0				L		I	L	L	
$C_3A + CaSO_4 \cdot 2D_2O$	10.00/ 1.72	93	5.5				L			L	L	
$C_{12}A_7 + CaSO_4 \cdot 2D_2O$	1.44/ 6.94	27	10.0			F		LX	L			X
$C_{12}A_7 + CaSO_4 \cdot \frac{1}{2}D_2O$	1.44/ 6.94	80	3.0		F			L	L			
$CA + CaSO_4 \cdot \frac{1}{2}D_2O$	12.66/ 6.94	80	11.0		F			L	L			
$CA + CaSO_4 \cdot \frac{1}{2}D_2O$	12.66/ 6.94	80→120	4.5					LX	L			

Table 2b.

Sample mixture	Ratios (mmols)	T (°C)	Total time (h)	$CaCO_3$	$C_4A\bar{C}D_{11}$	Int. phase	C_3AD_6	β-$Ca_4Al_2O_6Cl_2 \cdot 10D_2O$	SiO_2	$Ca(OD)_2$
$C_3A + CaCO_3$	5.56/15.00	53	2.3	FL	L					
$C_{12}A_7 + CaCO_3$	1.44/10.00	27	11.0	FLX	LX					
$C_{12}A_7 + CaCO_3$	1.44/10.00	53	5.0	FL	L	I				
$CA + CaCO_3$	11.65/11.60	53	11.0	FL	L					
$CA + CaCO_3$	11.65/11.60	80	9.5	FL	L		L			
$C_{12}A_7 + CaCO_3$	1.44/ 9.01	27	5.0					LX		
$C_3A + SiO_2$	1.44/16.65	80	1.3				L		FL	
$C_3A + Ca(OD)_2$	5.93/18.40	100	1.3				F			FL

Results

i) $CaSO_4 \cdot \frac{1}{2}D_2O$ and $CaSO_4 \cdot 2D_2O$ as additives

The extension of the CaO-Al_2O_3-D_2O system to four components by including SO_3 introduces the possibility of other hydration products than those of the three component system. Unfortunately, the D-atom positions of the sulphate containing phases, ettringite ($C_6A\bar{S}_3D_{32}$) and monosulphate ($C_4A\bar{S}D_{12}$) are not known. Hence, an immediate identification of these phases from the observed neutron diffraction powder patterns is difficult. In this study the effect of $CaSO_4 \cdot \frac{1}{2}D_2O$ and $CaSO_4 \cdot 2D_2O$ on the hydrolysis of C_3A, $C_{12}A_7$ and

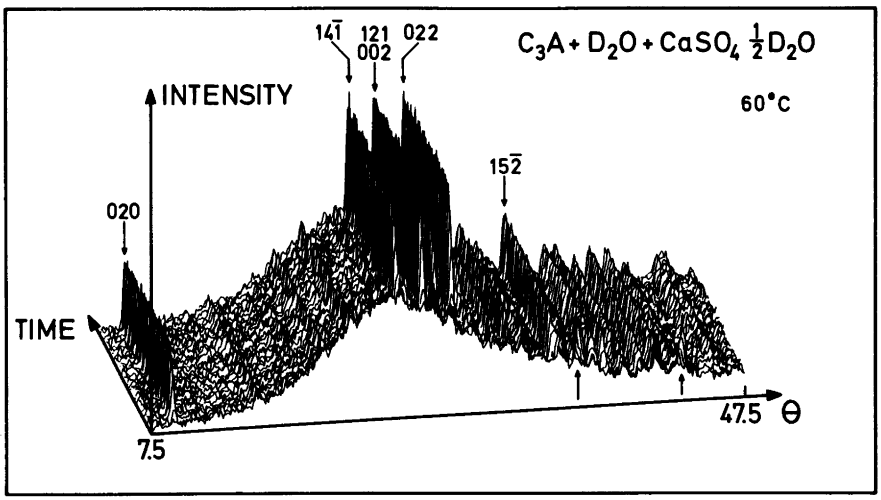

Fig. 1. Powder neutron diffraction patterns of a C_3A-$CaSO_4 \cdot \frac{1}{2}D_2O$-$D_2O$ mixture at 60 °C recorded with 5 min intervals. Selected Miller indices of $CaSO_4 \cdot 2D_2O$ ↓ and $CaSO_4 \cdot \frac{1}{2}D_2O$ ↑ are indicated.

CA was investigated for temperatures between 25 and 120 °C. The crystalline phases present in the first and the last on-line neutron diffraction pattern of the individual experiment series are listed in Table 2a, and the tabulated results conform reasonably well with earlier findings. Electron microscopy techniques[9] revealed that the first reaction product in the hydrolysis of calcium aluminates in the presence of gypsum is ettringite as long as the $CaSO_4 \cdot 2H_2O$ amount is sufficient for a quantitative reaction. Ettringite may itself after some time react with the remaining calcium aluminates to give monosulphate as a secondary product. However, at low sulphate concentrations it was found that monosulphate is the first crystalline reaction product.[9] The latter reaction product may also take compositions belonging to a solid solution phase between $C_4A\bar{S}D_{12}$ and C_4AD_{19}.[10]

No difference in crystalline end products was found when using $CaSO_4 \cdot \frac{1}{2}D_2O$ and gypsum, respectively, as additives (*cf.* Table 2a). At temperatures between room temperature and 70 °C $CaSO_4 \cdot \frac{1}{2}D_2O$ was found to react very fast with D_2O giving $CaSO_4 \cdot 2D_2O$ in agreement with the hydration properties of pure hemihydrate in the absence of calcium aluminates.[4] This hydration reaction did not take place at more elevated temperatures. Thermal decomposition of $CaSO_4 \cdot 2D_2O$ inside the vanadium container was found to give $CaSO_4 \cdot 0.8D_2O$,[4] which is not the same crystalline modification as the present starting material of hemihydrate ($CaSO_4 \cdot 0.67D_2O$).

a) Reactions with C_3A: The hydration of C_3A in the presence of $CaSO_4 \cdot \frac{1}{2}D_2O$ was first studied at 60 °C. The adopted ratio (calcium aluminate/additive) of 4.26/12.85 mmols is considerably smaller than in real Portland cement. The time variation of the recorded powder neutron diffraction patterns is visualized in Fig. 1 showing diffraction patterns recorded at 5 min intervals. Immediately (5 min) after the solid mixture has been brought into contact with water, the diffraction pattern consists of only faint Bragg reflections and a broad background peak, indicating loss of crystallinity of C_3A and $CaSO_4 \cdot \frac{1}{2}D_2O$. From the variations in integrated intensities of Bragg reflections ascribed to the different phases information concerning the reaction rates was obtained. This is illustrated in Fig. 2b. These results can in turn be compared with the corresponding data for the hydration of pure C_3A and pure $CaSO_4 \cdot \frac{1}{2}D_2O$. Complete transformation of $CaSO_4 \cdot \frac{1}{2}D_2O$ into gypsum (Fig. 2b) was found within 25 min which is faster than for the pure $CaSO_4 \cdot \frac{1}{2}D_2O$ sample itself (1 h).[4] C_3AD_6, which is normally the hydration product[1,2] of pure C_3A, is not at all formed under these conditions. Instead two strong additional reflections in the powder patterns were recognized and ascribed

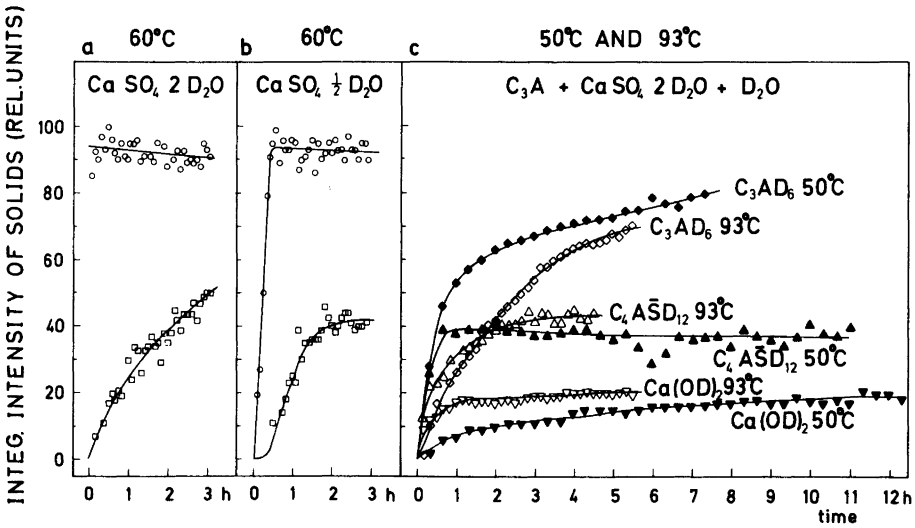

Fig. 2. Integrated intensities of solids from reactions of C_3A-D_2O mixtures with additives $CaSO_4 \cdot 2D_2O$ and $CaSO_4 \cdot \frac{1}{2}D_2O$; a and b at 60 °C and c at 50 and 93 °C. The solids observed are $CaSO_4 \cdot 2D_2O$ (○), precursor (□), C_3AD_6 (◆,◇), $C_4A\bar{S}D_{12}$ (▲,△), and $Ca(OD)_2$ (▼,▽).

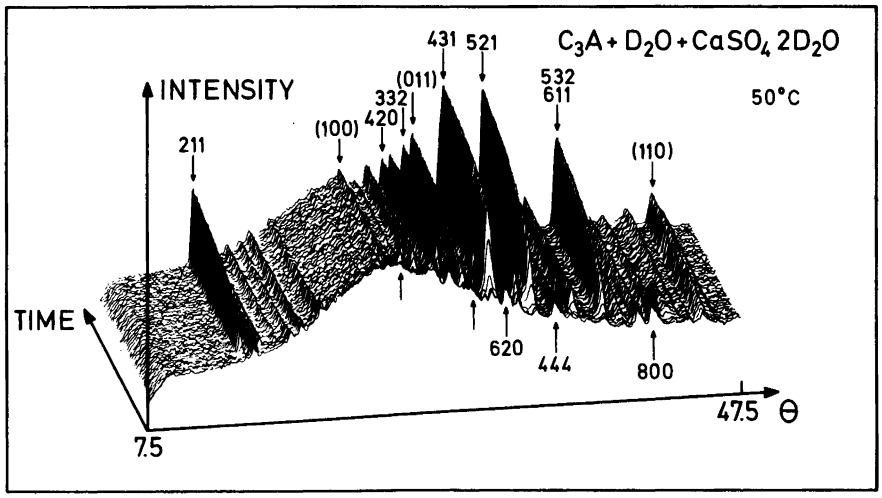

Fig. 3. Powder neutron diffraction patterns of a C_3A-$CaSO_4 \cdot 2D_2O$-D_2O mixture at 50 °C recorded with 5 min intervals. Selected Miller indices of C_3AD_6 ↓, $Ca(OD)_2$ ↓ (*hkl*), and C_3A ↑ are indicated. The positions of two reflections from the precursor are marked with ↑. The two strong reflections of the precursor can be indexed with the ettringite unit cell as 124 and 216.

(see below) to a precursor for $C_6A\bar{S}D_{32}$. Fig. 2b shows the time dependence of the amount of this precursor. A similar experiment with C_3A at 60 °C using $CaSO_4 \cdot 2D_2O$ as additive revealed the same features, and the results are shown in Fig. 2a. Again, no C_3AD_6 was formed. These results showing the appearance of the precursor phase are in contrast to the reported observations that

$C_6A\bar{S}D_{32}$ is the first crystalline product in the hydrolysis of Portland cement (mortars which generally contains gypsum as well as the hemihydrate).[3,10] In an experiment at 50 °C a C_3A to $CaSO_4 \cdot 2D_2O$ ratio of 10.00/1.72 mmol was chosen (Fig. 2c). This ratio is closer to that used in Portland cement than the ratios used in the experiments described above. Under these conditions, quite different hydrolysis reactions were observed than those described above at 60 °C. The time dependence of the diffraction patterns is shown in Fig. 3. All the available gypsum is consumed in the very beginning, and the crystalline reaction products are identified as C_3AD_6, $Ca(OD)_2$ and $C_4A\bar{S}D_{12}$ from the positions of the diffraction lines. In addition, the precursor appears as an intermediate phase during the first hour of hydration. An analogous experiment was performed at 93 °C yielding the same reaction products, however, with the exception that the precursor phase was not observed. The variations in integrated intensities *versus* time for reflections characteristic of these phases (at 50 and 93 °C) are shown in Fig. 2c.

None of the described experiments showed indication of the formation of ettringite. A $C_3A/CaSO_4 \cdot 2D_2O$ mixture (ratio 10.00/1.72 mmols) was studied at room temperature in order to check whether this, somewhat surprising, finding was maintained. The time variation of the diffraction patterns (*cf.* Fig. 4) differs from those presented in Figs. 1 and 3. During the first 8 h the precursor is the only crystalline reaction product. However, after 8 h, precipitation of ettringite takes place accompanied by a simultaneous consumption of C_3A and of the precursor. Time variations of the integrated intensities are shown in Fig. 5a. After the on-line experiment the sample was kept in the sample holder for 80 days at room temperature and then subjected to X-ray powder diffraction measurements (on the wet paste). The reaction products were now found to be C_3AD_6 and $C_4A\bar{S}D_{12}$. They are probably the stable reaction products.

In order to identify the precursor unequivocally in this and the other experiments involving sulphate additives, further experiments were performed using X-ray diffraction on $C_3A/CaSO_4 \cdot 2H_2O$ samples (ratio 8.51/21.24 mmols, water/solid ratio 1.27). The reaction temperature was 60 °C, and diffraction patterns of the wet samples were recorded after 1, 2, 3, 5, 10, 17, and 30 h. However, surprisingly, only ettringite, in quantities increasing with the reaction time, was observed, in contrast to the observations made by on-line powder neutron diffraction.

It proved to be possible to synthesize the precursor in a hydrothermal experiment. A mixture

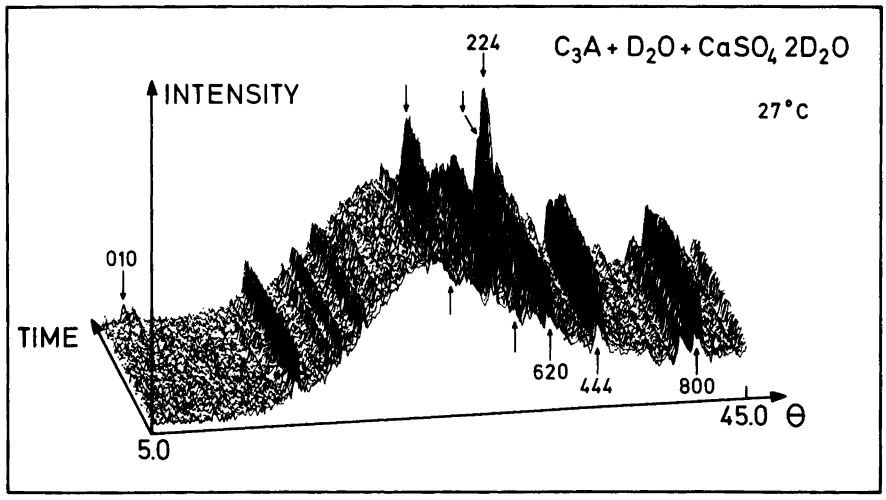

Fig. 4. Powder neutron diffraction patterns of a C_3A-$CaSO_4 \cdot 2D_2O$-D_2O mixture at 27 °C recorded with 10 min intervals. Selected Miller indices of C_3A ↑ and $C_6A\bar{S}D_{32}$ ↓ and positions of two reflections of the precursor ↓ and ↑.

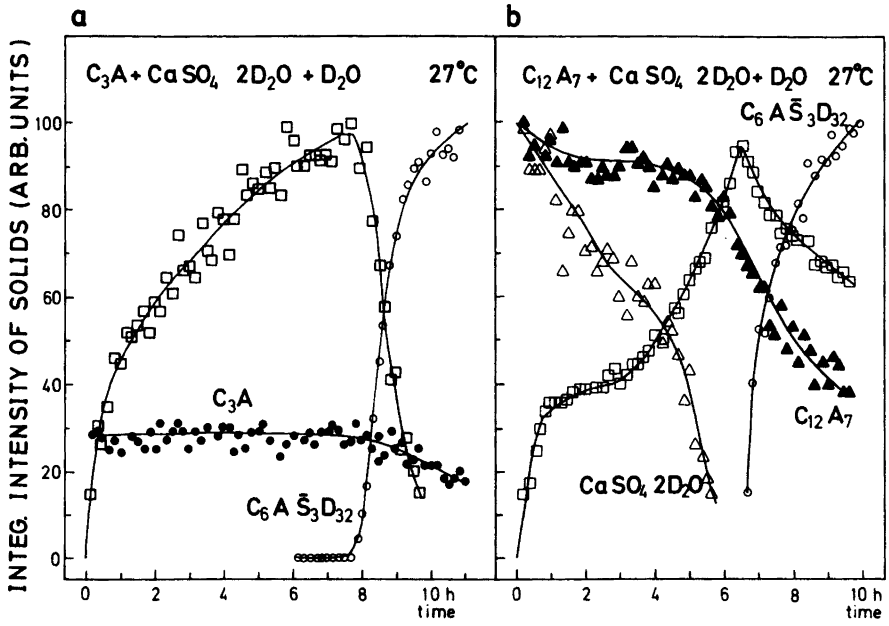

Fig. 5. Integrated intensities of solids in reactions of a: C_3A-$CaSO_4 \cdot 2D_2O$-D_2O mixtures at 27 °C and b: $C_{12}A_7$-$CaSO_4 \cdot 2D_2O$-D_2O mixtures at 27 °C. The precursor is represented by □.

of 13.3 mmol C_3AD_6, 41 mmol $CaSO_4 \cdot \frac{1}{2}D_2O$, and 150 ml D_2O was kept at 150 °C for 100 h. Guinier photographs of the end product showed only sharp lines of orthorhombic anhydrite $CaSO_4$. However, after 250 days at room-temperature, renewed X-ray diffraction investigations revealed the coexistence of anhydrite and ettringite (data in full accordance with JCPDS index data[11]), and the presence of a few, weak unidentified Bragg reflections. (The refined unit cell dimensions of hexagonal ettringite are a = 11.242(4) and c = 21.479(13) Å.) Remarkably, the neutron diffraction pattern obtained after 250 d did *not* show significant changes with respect to the earlier recorded data. A high temperature powder X-ray diffraction study (Guinier Simon camera) was undertaken with the anhydrite/ettringite mixture for temperatures between 25 and 825 °C. Whereas ettringite was found to decompose at 125 ± 10 °C, the reflections of anhydrite remained up to 825 °C. No phase transition of ettringite could be detected between 25 and 125 °C. As evident from Fig. 5a, b (and from experiments described below) the quantities of the precursor phase and ettringite are in some way linked together. These facts were taken as an indication that the precursor phase may be a metastable modification of ettringite with different positioning of the OD^- and D_2O groups. Table 3 gives the d-spacings and estimated intensities for the Bragg reflections observed for the precursor (characterized at d = 3.02 and 2.56 Å) and ettringite (characterized at d = 9.61 and 2.47 Å) in the powder neutron diffraction diagrams. The *hkl* values for the ettringite reflections are included. However, it was also possible to index the diffraction pattern of the precursor phase on the ettringite type unit cell and no common (strong) reflections for the two phases were present (*cf.* the indexing of the precursor phase also included in Table 3). From these findings, it is believed that ettringite can exist in two modifications, which mainly differ in the OD^-/D_2O geometry (or their amounts), and are not distinguishable in powder X-ray diffraction diagrams. Single crystal neutron diffraction studies are required in order to definitely solve the problem.

b) Reactions with $C_{12}A_7$ and CA: For pure $C_{12}A_7$ the hydration product at temperatures up to 30 °C is C_2AD_6, while for pure CA below 50 °C

Table 3. Observed positions (*d*-values), intensities and suggested indexing (*hkl*) of observed Bragg reflections of the precursor and ettringite in powder neutron diffraction diagrams.[a]

Precursor			Ettringite		
d(Å)	*hkl*	Int.	*d*(Å)	*hkl*	Int.
5.35	004	4	9.61	100	7
4.95	112	4	4.67	104	8
3.66	210	4	2.90	107	32
3.60	204	9	2.746	304	44
3.24	300	9	2.469	224	100
3.16	301	4	2.391	314	22
3.02	124	63	2.353	402	40
2.92	017	5	2.310	109	19
2.81	220	26	2.283	403	34
2.78	125	14	2.140	136	26
2.72	222	35	2.049	234	10
2.62	312	14	1.877	236	11
2.565	216	100	1.847	331	7
2.355	127	28			
2.310	109	44			
2.290	043	10			
2.218	037	31			
2.162	128	17			

a) Based on hexagonal unit cell with a = 11.19(1), c = 21.42(4) Å.

the hydration product is C_3AD_{12}.[1] These hydrates, also including C_2AD_8 and CAD_{10}, are metastable with respect to C_3AD_6. The slow transformation of these into the stable form is connected with large volume contractions and hence mechanical breakdown of the solidified cement mortar. However, in the room temperature hydrolysis of $C_{12}A_7$ and CA when using $CaSO_4 \cdot 2D_2O$ as additive (ratios 1.44/6.94 and 12.66/6.94 mmols, respectively), the formation of the metastable hydrates was suppressed.

The evolution of the diffraction patterns at 27 °C with time is shown for the $C_{12}A_7$ sample in Fig. 6 while integrated intensities are presented in Fig. 5b. It is seen that ettringite first starts to be precipitated when all gypsum is consumed, and that this correlated with the time when maximal amounts of the precursor are present in the sample. After another 80 days at room temperature, powder X-ray diffraction data recorded on the wet paste showed the presence of ettringite and α-C_4AD_{19}. The possible conversion of ettringite to $C_4A\bar{S}D_{12}$, due to low amounts of sulphate (*cf.* Table 2a), had not taken place.

The results from a similar experiment at 80 °C with $CaSO_4 \cdot \frac{1}{2}D_2O$ as additive, are presented in fig. 7a. At this elevated temperature gypsum is no longer formed from $CaSO_4 \cdot \frac{1}{2}D_2O$, but the reaction products are still the precursor and et-

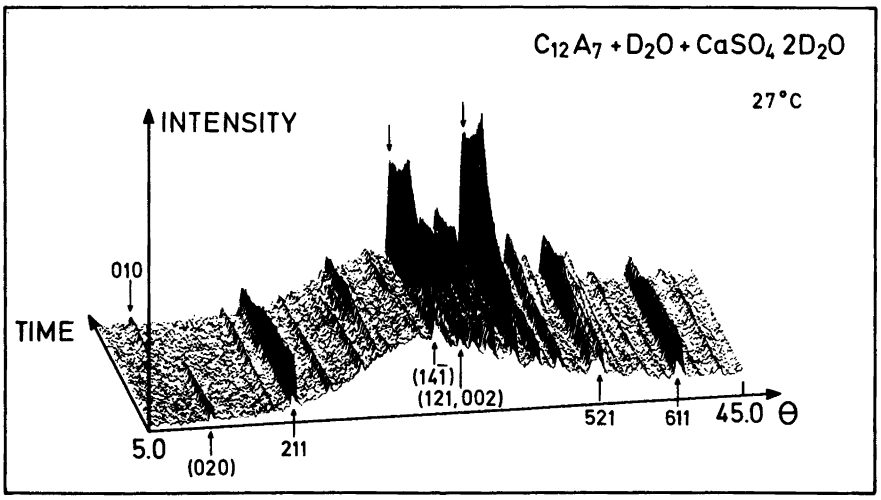

Fig. 6. Powder neutron diffraction patterns of $C_{12}A_7$-$CaSO_4 \cdot 2D_2O$-D_2O mixture at 27 °C recorded with 10 min intervals. Selected Miller indices of $C_{12}A_7$ ↑, $CaSO_4 \cdot 2D_2O$ ↑ (*hkl*), and $C_6A\bar{S}D_{32}$ ↓, and positions of two reflections from precursor ↓.

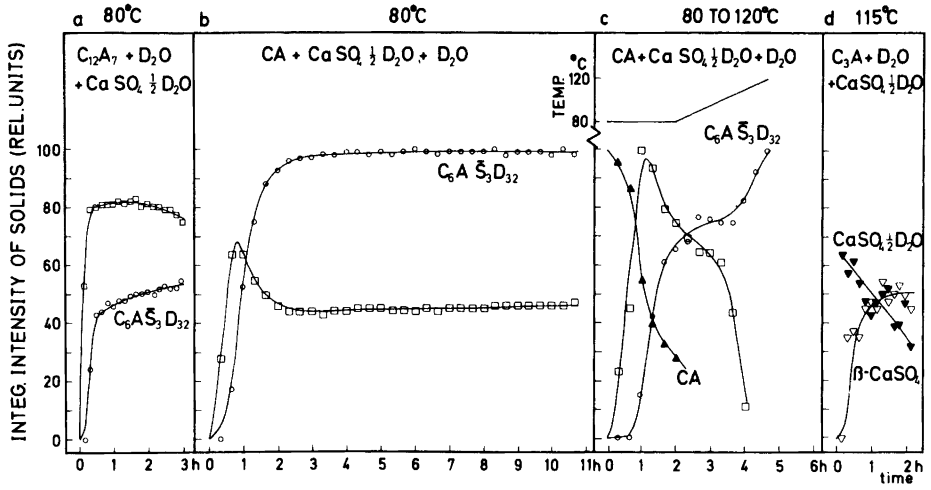

Fig. 7. Integrated intensities of solids in reactions of a: $C_{12}A_7$-$CaSO_4 \cdot \frac{1}{2}D_2O$-$D_2O$ at 80 °C, b: *CA*-$CaSO_4 \cdot \frac{1}{2}D_2O$-$D_2O$ at 80 °C, c: *CA*-$CaSO_4 \cdot \frac{1}{2}D_2O$-$D_2O$ at 80 to 120 °C, and d: C_3A-$CaSO_4 \cdot \frac{1}{2}D_2O$ at 115 °C. The precursor is represented by □.

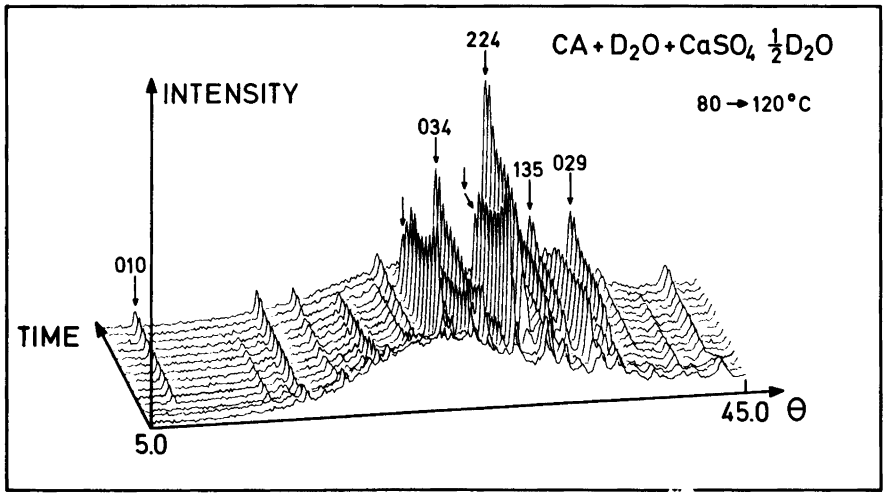

Fig. 8. Powder neutron diffraction diagrams of a mixture of *CA*-$CaSO_4 \cdot \frac{1}{2}D_2O$-$D_2O$ under heating from 80 to 120 °C. Diagrams were recorded with 20 min intervals. Selected Miller indices of reflections of $C_6A\bar{S}D_{32}$ ↓, and positions of two reflections of the precursor ↓.

tringite. X-Ray powder diffraction data on the end product confirmed the presence of ettringite. Corresponding data for a *CA*/$CaSO_4 \cdot \frac{1}{2}D_2O$ mixture are presented in Fig. 7b, and the reaction features were found to be identical with those described above.

Ettringite can be obtained from aqueous solutions up to 90 °C,[12] whereas $C_4A\bar{S}D_{12}$ is stable even at higher temperatures. In order to get some information on the thermal stability of the sulphate containing hydration products under the present experimental conditions a sample of

D_2O, *CA*, and $CaSO_4 \cdot \frac{1}{2}D_2O$ (ratio 12.66/6.94 mmols) was kept for 2 h at 80 °C before slowly being heated up to 120 °C over 4 h. The time variations of the recorded on-line powder neutron diffraction patterns are shown in Fig. 8, and the evaluated variation in integrated intensities in Fig. 7c. The formation of ettringite continued to take place even at 120 °C. Powder X-ray diffraction data of the sample confirmed after 80 days at room temperature still the presence of ettringite. On the other hand, in a hydration experiment of C_3A with $CaSO_4 \cdot \frac{1}{2}D_2O$ as additive (ratio 4.26/12.85 mmols) at 115 °C no ettringite nor any precursor phase was found. The hemihydrate was partially converted to orthorhombic anhydrite, β-$CaSO_4$,[13] see Fig. 7d, while no other reaction products were registered.

ii) $CaCO_3$ as additive

In the system CaO-Al_2O_3-CO_2-D_2O the phases $3CaO \cdot Al_2O_3 \cdot CaCO_3 \cdot 30D_2O$ and $3CaO \cdot Al_2O_3 \cdot CaCO_3 \cdot 11D_2O$ are well known. The compound $C_4A\bar{C}H_{11}$ is formed when calcite is used as an additive in Portland cement mortars.[14] Another carbonate, $4CaO \cdot Al_2O_3 \cdot \frac{1}{2}CO_2 \cdot 12H_2O$, can appear as an intermediate phase when insufficient quantities of $CaCO_3$ are present for the formation of $C_4A\bar{C}H_{11}$.[15] In the present experiments only $C_4A\bar{C}D_{11}$ was found as the end product. The molar ratios between the amounts of calcium aluminates and $CaCO_3$ used are listed in Table 2b. For the $C_3A/CaCO_3$ mixture $CaCO_3$ is in excess while the other mixtures have a CaO deficiency with respect to the formation of $C_4A\bar{C}D_{11}$.

The time dependence of the diffraction patterns of a $C_3A/CaCO_3$ mixture at 53 °C is shown in Fig. 9. C_3A reacts rapidly with water and the crystalline reaction product is $C_4A\bar{C}D_{11}$. The variation of integrated intensities with time are shown in Fig. 10a. During the time period of the experiment some 40 % consumption of the available amount of $CaCO_3$ takes place. This implies that most of the initial C_3A remains in the amorphous state even after 2 h. Analogous observations were made for the hydration of $C_{12}A_7$ in the presence of $CaCO_3$. However, the consumption rate of $CaCO_3$ was lower than in the experiment with C_3A. The variations of integrated intensities with time in the latter experiment are shown in Fig. 10b. An X-ray diffraction powder pattern recorded of the wet specimen after 80 days at room temperature proved that it contained only $C_4A\bar{C}D_{11}$ and $CaCO_3$. Similar findings were also obtained for an on-line study of a $CA/CaCO_3$ mixture, the results being presented in Fig. 10c. The amount of $CaCO_3$ is constant after 6 h (Fig.

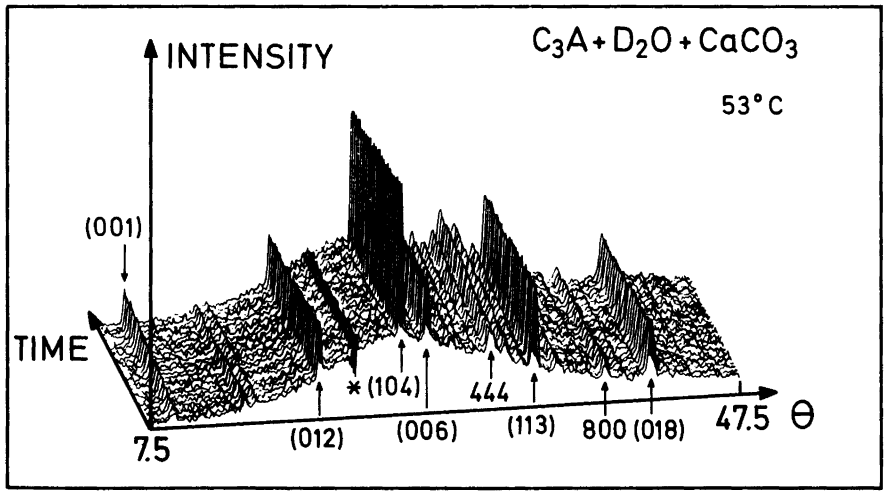

Fig. 9. Powder neutron diffraction patterns of a C_3A-$CaCO_3$-D_2O mixture at 53 °C recorded with 5 min intervals. The "peak" marked * is due to instrumental instability. Miller indices of selected reflections of C_3A ↑, $CaCO_3$ ↑ (*hkl*), and $C_4A\bar{C}D_{11}$ ↓ (*hkl*) are indicated.

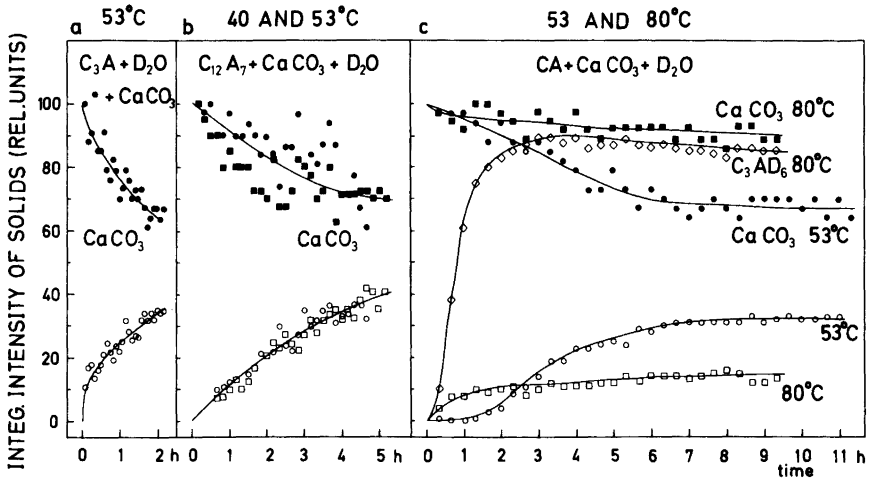

Fig. 10. Integrated intensities of solids in reactions of a: C_3A-$CaCO_3$-D_2O at 53 °C, b: $C_{12}A_7$-$CaCO_3$-D_2O at 40 and 53 °C, and c: CA-$CaCO_3$-D_2O at 53 and 80 °C. The compound $C_4A\bar{C}D_{11}$ is represented by ○ and □.

10c). This corresponds to a quantitative conversion of CA to $C_4A\bar{C}D_{11}$, in contrast to the findings for C_3A and $C_{12}A_7$.

The reaction between CA, $CaCO_3$, and D_2O was studied also at the higher temperature of 80 °C. The results differ clearly from those at 53 °C in that C_3AD_6 is formed in addition to $C_4A\bar{C}D_{11}$, as seen in the powder diffraction diagrams of Fig. 11. The variations in integrated intensities with time are included with the 53 °C data in Fig. 10c. The major hydration products at 80 °C is C_3AD_6. Both at 53 and 80 °C large amounts of A remain as an amorphous gel. It can be concluded that the suppression effect on the C_3AD_6 formation induced by $CaCO_3$ additions, apparently has an upper temperature limit in the range 53–80 °C.

By a careful study of the diffraction patterns

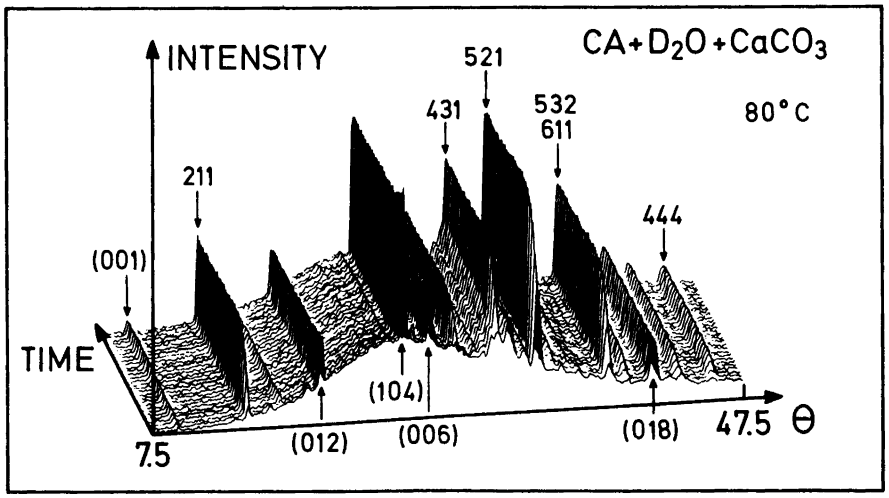

Fig. 11. Powder neutron diffraction patterns of a mixture of CA-$CaCO_3$-D_2O at 80 °C, recorded with 20 min intervals. Selected Miller indices of $CaCO_3$ ↑ (*hkl*), C_3AD_6 ↓, and $C_4A\bar{C}D_{11}$ ↓ (*hkl*) are indicated.

from *e.g.* $C_{12}A_7/CaCO_3$ mixtures at 53 °C, an intermediate phase is observed. Maximum amount of this phase is attained after ~40 min, and it has completely disappeared after 3–4 h. Unfortunately, only two Bragg reflections could be unequivocally ascribed to this phase, thereby making an identification impossible. These reflections were tentatively ascribed to $C_4A\bar{C}_{0.5}D_{12}$ that has a Bragg reflection at d = 2.722 Å.[15]

For the pure systems (*viz.* without additives) the reaction rates for C_3A are greater than those of $C_{12}A_7$, while CA is the slowest reactant. This picture is changed when $CaCO_3$ is used as additive; the reaction of CA is here more rapid than that of $C_{12}A_7$. This may, however, be due to differences in surface area/particle size since *e.g.* the preparation methods here adopted differ for the latter two phases.

iii) $Ca(OD)_2$ as additive

Portland cement clinker often contains minor amounts of free CaO[16] and $Ca(OH)_2$ is sometimes added to the mortars. As described in Ref. 2, $Ca(OD)_2$ is produced during the hydrolysis of C_3S. A possible influence of $Ca(OD)_2$ on the hydrolysis of calcium aluminates was here briefly considered through one experiment involving C_3A. The reaction between D_2O and a sample of C_3A containing a surplus of $Ca(OD)_2$ was studied by on-line powder neutron diffraction (ratio 5.93/18.40 mmols, temperature 100 °C). As seen from the diffraction patterns presented in Fig. 12, C_3AD_6 is formed almost immediately. This corresponds the the findings for pure C_3A, and the reaction rate of C_3A seems not to be affected by the presence of $Ca(OD)_2$.

iv) SiO_2 as additive

An experiment with a $C_{12}A_7/SiO_2$ mixture (ratio 1.44/16.65 mmols) was carried out at 85 °C. No *C-S-D* phases were formed, nor did the presence of SiO_2 significantly alter the rate of hydrolysis of $C_{12}A_7$. The only crystalline hydration product was C_3AD_6.

v) $CaCl_2$ as additive

In the monitoring of cement setting properties, additives such as *e.g.* $CaCl_2$, $Ca(NO_3)_2$ or CaI_2 can also be used.[17,18] One experiment with $C_{12}A_7$ and $CaCl_2$ (ratio 1.44/9.01 mmols) was performed at room temperature. Immediately after mixing, a large heat evolution was observed mainly due to the reaction of $CaCl_2$ with water. Signs of a Ca-Cl phase in the powder diagrams were first seen after an induction period of ~30 min. The final crystalline end product was found to be β-$Ca_4Al_2O_6Cl_2 \cdot 10D_2O$. After 80 days at room

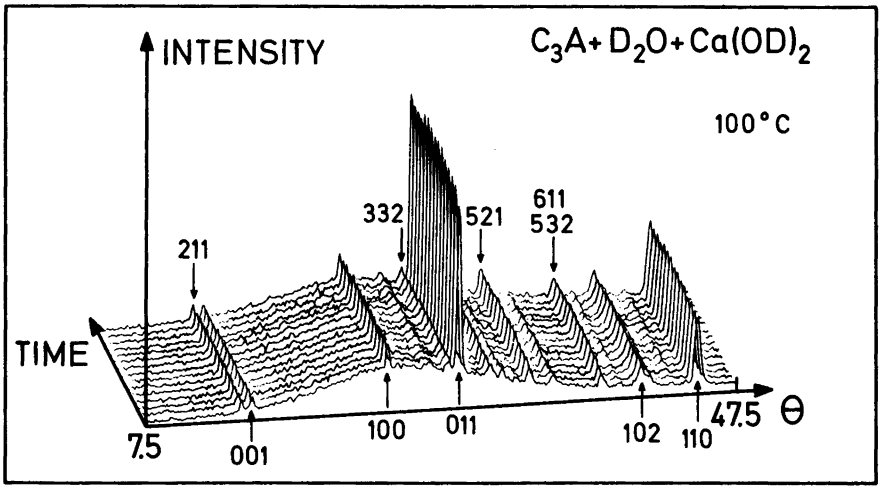

Fig. 12. Powder neutron diffraction patterns of a C_3A-$Ca(OD)_2$-D_2O mixture at 100 °C recorded with 5 min intervals. Selected Miller indices of $Ca(OD)_2$ ↑ and C_3AD_6 ↓ are indicated.

temperature the wet sample showed only lines from this phase (X-ray powder diffraction). The experiment was repeated and X-ray powder patterns of the wet samples were recorded after 1, 3, 5, and 28 h. After 5 h the reflections of β-$Ca_4Al_2O_6Cl_2 \cdot 10H_2O$ appeared.[19]

vi) Background scattering

The free liquid D_2O gives rise to a scattering contribution that contains a very broad peak in the middle of the recorded diagrams. Information about the amount of free D_2O can thus be obtained from integration of a section of this peak. The variations in free D_2O *vs.* time were evaluated for the experiments described in *i*)–*v*), and representative curves are shown in Fig. 13. A common feature of these diagrams is the strong reduction of the free D_2O amount during the initial part of the experiments. The D_2O consumptions should be compared with the dissolution processes of the crystalline reactants and the precipitation of crystalline products, see *e.g.* Figs. 2, 5, 7, and 10. In general, the initial, fast reduction in free D_2O amount does not correspond to the crystallization of hydrated products, and is hence ascribed to the rapid conversion of reactants into amorphous gels. Further along in the reactions, correlations between rate of crystallization and consumption of D_2O are observed. This is seen by *e.g.* comparing the results for the $CA/CaCO_3$ sample at 53 °C in Figs. 10c and 13, and the rate of crystallization of $C_4A\bar{C}D_{11}$ is well reflected in the curve showing the variation in the free amount of water. In the insert to Fig. 13 the crystalline amount of $C_4A\bar{C}D_{11}$ is plotted *vs.* the consumption of water, and a linear relation is present. In this case, the reference quantity of D_2O is that observed after 1 h. However, in order to give a full account of the variation in amount of free water *versus* time, improved time resolution is required so that results can also be obtained for the first minutes.

Discussion

The hydration reactions of pure calcium aluminates as studied by powder neutron diffraction

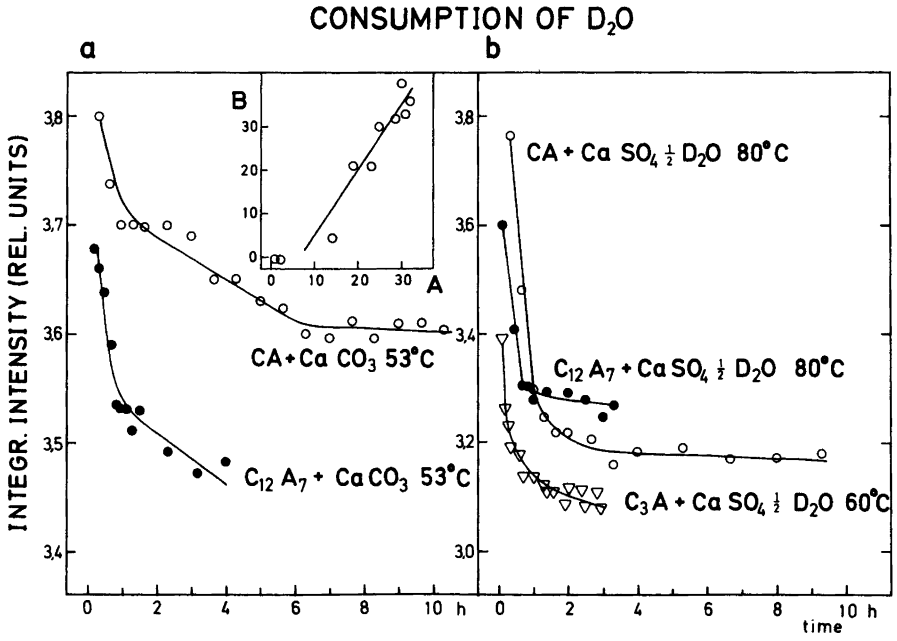

Fig. 13. Consumption of D_2O in selected hydrolysis reactions, a for $CaCO_3$ and b for $CaSO_4 \cdot \frac{1}{2}D_2O$ as additive. The insert shows B the consumption of D_2O (integrated intensity in arbitrary units) *vs.* A the production of $C_4A\bar{C}D_{11}$ (integrated intensity in arbitrary units).

were reported in Refs. 1,2. The results of the present experiments which are concerned with the effects of additives, differ in many ways from the results obtained for the pure phases. The most apparent feature is the formation of different crystalline reaction products where the additive anions are incorporated in the crystal structure. These complex hydration products generally crystallize in layer structures (*e.g.* $[Ca_2Al(OD)_6][\frac{1}{2}X \cdot nD_2O]$ with X = Cl, SO_4, *etc.* and n = 10–12)[17,18] often with large repetition lengths, and the details of the crystal structures are only partly known. The formation of metastable crystalline *C-A-D* phases is prevented by the use of additives. For carbonate containing samples the stable product is $C_4A\bar{C}D_{11}$, at least at temperatures below ~80 °C. However, for sulphate containing specimens a much more complicated nature was found, *cf.* Table 2a. For all such samples studied, independent of the $C/\bar{S}$ ratio, a precursor was found as the primary reaction product. In the literature,[20] ettringite, $C_6A\bar{S}_3H_{32}$, is quoted as the first occurring crystalline $\bar{S}$ containing phase, and no reference has been found for a precursor of ettringite. However, this is possibly the first time that these systems have been studied by the powder neutron diffraction technique which yield information about the scattering contributions from the deuterium atoms. It is here suggested that the precursor is a metastable form of ettringite, and that the transformation from the precursor to ettringite is mainly driven by rearrangement of the deuterium atoms. Such a (minor) rearrangement will be observed in a neutron diffraction experiment, but the effect could possibly hardly be detected in X-ray powder diffraction measurements. Another possibility is that the precursor has a composition (slightly) different from that of ettringite and that complete hydration first takes place in the second step.

The formation of ettringite takes place after the crystalline amount of the precursor has reached its maximum and is in most cases connected with a reduction in quantity of the precipitated precursor. After prolonged reaction times (at room temperature) another transformation to $C_4A\bar{S}D_{12}$ and C_3AD_6 was observed in some cases while α-C_4AD_{19} was found in another case. Hence the reaction products for the systems containing sulphate varies largely and these findings should be checked by prolonged on-line diffraction experiments. The absence of any crystalline Al-O-D phase (*e.g.* gibbsite)[21,22] in all the experiments performed is somewhat unexpected. However, the quantities of gibbsite may have been so small that they could not be detected from the diffraction patterns.

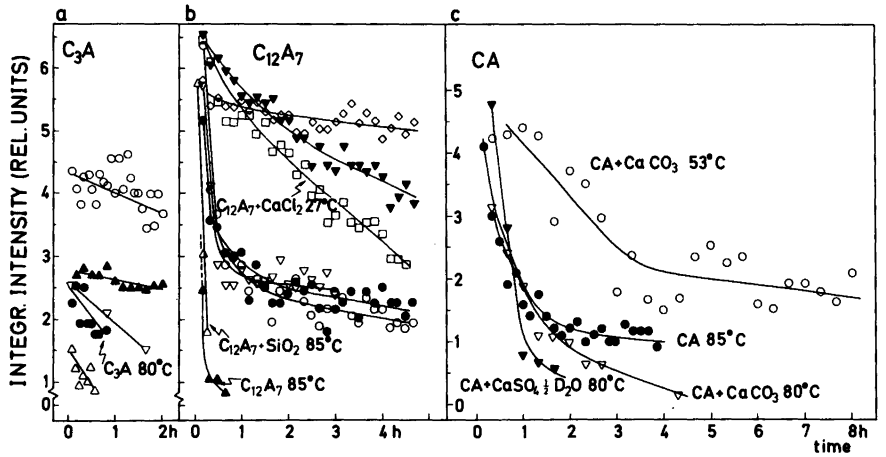

Fig. 14. Integrated intensities *versus* time for initial reactions of C_3A-. $C_{12}A_7$- and *CA*-D_2O-additive mixtures. The symbols represent the following additives:
a: $CaSO_4 \cdot \frac{1}{2}D_2O$ at 60 °C (○), $CaSO_4 \cdot 2D_2O$ at 60 °C (▽), $CaSO_4 \cdot 2D_2O$ at 27 °C (▲), and $CaCO_3$ at 53 °C (△).
b: $CaSO_4 \cdot \frac{1}{2}D_2O$ at 80 °C (▽), $CaSO_4 \cdot 2D_2O$ at 27 °C (◇), $CaCO_3$ at 53 °C (○,●), and $CaCO_3$ at 27 °C (▼).
c: All systems are identified on the figure.

Table 4. Estimated values for $t_{0.5}$ (product) in min for hydration reactions of *C-A* phases in the presence of additives.

C-A					Pure system	
	Additive	Product	Temp (°C)	$t_{0.5}$	$t_{0.5}$	Product
C_3A	$CaSO_4 \cdot \frac{1}{2}D_2O$	$CaSO_4 \cdot 2D_2O$	60	15	7	C_3AD_6
		Precursor		60		
	$CaSO_4 \cdot 2D_2O$	Precursor	60	>80	7	C_3AD_6
	$CaSO_4 \cdot 2D_2O$	C_3AD_6	50	40	17	C_3AD_6
		Precursor		15		
		$Ca(OD)_2$		>100		
	$CaSO_4 \cdot 2D_2O$	C_3AD_6	93	100	4	C_3AD_6
		Precursor		30		
		$Ca(OD)_2$		15		
	$CaSO_4 \cdot 2D_2O$	Precursor	27	60	70	C_3AD_6
	$CaCO_3$	$C_4A\bar{C}D_{11}$	53	>35	17	C_3AD_6
$C_{12}A_7$	$CaSO_4 \cdot \frac{1}{2}D_2O$	Precursor	80	7	6	C_3AD_6
		Ettringite		23		
	$CaCO_3$	$C_4A\bar{C}D_{11}$	53	>120	120	C_3AD_6
CA	$CaSO_4 \cdot \frac{1}{2}D_2O$	Precursor	80	25	30	C_3AD_6
		Ettringite		60		
	$CaCO_3$	C_3AD_6	80	50	30	C_3AD_6
		$C_4A\bar{C}D_{11}$		>60		
	$CaCO_3$	$C_4A\bar{C}D_{11}$	53	>200	>200	C_3AD_6

The reactivities of the calcium aluminates were characterized by the time $t_{0.5}$ necessary for consumption of half the initial amount of the reactant.[2] The reactivity of pure C_3A is so large that $t_{0.5}$ cannot be estimated by the present time resolution ($t_{0.5}$ being less than 0.1 h). This picture is not altered by the use of additives (Fig. 14a), hence, the results shown for C_3A in Fig. 14 correspond to minor amounts of C_3A reacting slowly due to particle size effects. However, for $C_{12}A_7$ and CA the hydration reactions are slower and can be evaluated. The reaction rates are not found to be lowered by the presence of additives, see Fig. 14 and Table 4 of Ref. 1. These fast hydration reactions correlates with the reduction of the amounts of free water as illustrated in Fig. 13.

Another feature of the reactivity of these solids is the rate at which crystalline products are formed. For the pure *C-A* systems $t_{0.5}$ (reactant) and $t_{0.5}$ (product) differ only slightly.[2] However, for the systems containing additives the formation of products is considerably slowed down, and $t_{0.5}$ (product) $> t_{0.5}$ (reactant). When compared with the pure systems, see Table 4, $t_{0.5}$ (product) for the systems containing additives is in most cases found to be larger than for the corresponding pure systems. The curves showing the degree of hydration [$\alpha(t)$] *versus* time contain information about the underlying kinetic relationships.[2] This aspects is not further considered here. However, their rather different profiles should be noted, *cf. e.g.* Figs. 2, 5, 7, and 10.

As a byproduct of these studies, information on the hydration reactions of $CaSO_4 \cdot \frac{1}{2}D_2O$ in the presence of *C-A* phases were obtained. The consumption of $CaSO_4 \cdot \frac{1}{2}D_2O$ *versus* time is shown in fig. 15. The reactions are found to be fastest at low temperatures in conformity with data for pure $CaSO_4 \cdot \frac{1}{2}D_2O$.[4] For the hydration curves shown in Fig. 15 different reaction products prevail; $CaSO_4 \cdot 2D_2O$ at 60 °C, the precursor and ettringite at 80 °C, and orthorhombic β-$CaSO_4$ at 115 °C. The hydration of $CaSO_4 \cdot \frac{1}{2}D_2O$ in the presence of C_3A at 60 °C to yield gypsum can be compared with corresponding data for pure $CaSO_4 \cdot \frac{1}{2}D_2O$.[4] In the latter case, the hydration curve, $\alpha(t)$, takes a sigmoidal form and different mechanisms such as crystallization of nuclei, dissolution and diffusion have been suggested to determine the reaction rates at different stages of

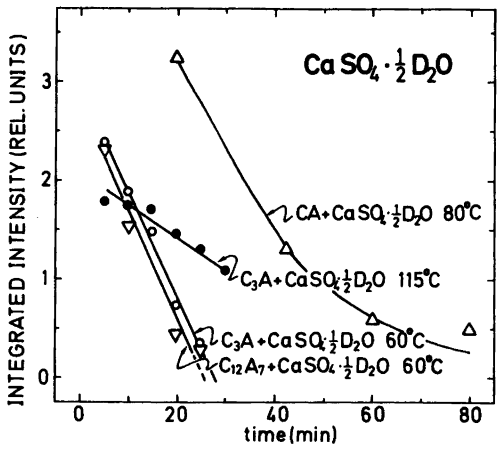

Fig. 15. Integrated intensity of $CaSO_4 \cdot \frac{1}{2}D_2O$ *vs.* time showing the rate of consumption at different experimental conditions.

the process. However, in the presence of C_3A the degree of hydration of $CaSO_4 \cdot \frac{1}{2}D_2O$ varies linearly with time (see Fig. 2).

Acknowledgements: Support for this investigation was granted by *The Danish Natural Science Research Council* (ANC), and by *The Royal Norwegian Council for Scientific and Industrial Research* (HF). Mr. N. J. Hansen is thanked for his assistance in the preparation of the specimens used in the investigation.

References

1. Christensen, A. N. and Lehmann, M. S. *J. Solid State Chem. 51* (1984) 196.
2. Christensen, A. N., Fjellvåg, H. and Lehmann, M. S. *Acta Chem. Scand. A* (in press).
3. Bensted, J. *Cem. Concr. Res. 13* (1983) 493.
4. Christensen, A. N., Lehmann, M. S. and Pannetier, J. *J. Appl. Cryst.18* (1985) 170.
5. Bushuev, N. N. and Borisov, V. M. *Russ. J. Inorg. Chem. 27* (1982) 341.
6. Breval, E. *Cem. Concr. Res. 6* (1976) 129.
7. Wolfers, P. *Programs for Treatment of Powder Profiles,* ILL, Grenoble (1975), personal communication.
8. Yvon, K., Jeitschko, W. and Parthé, E. *J. Appl. Cryst. 10* (1977) 73.
9. Locher, F. W., Reichartz, W., Sprung, S. and Rechenberg, W. *Zem. Kalk-Gips Ed. B 36* (1983) 3.
10. Agdel Razig, B. E. I., Parker, K. M. and Sharp, J. H. *Therm. Anal. Proc. Int. Conf. 7th I* (1982) 571.
11. JCPDS data card No. 31-251.
12. Lieber, W. *Zement-Kalk-Gips* (1963) 364.
13. JCDPS data card No. 6-226.
14. Henning, O. and Kudjakow, A. *Wiss. Z. Hochsch. Archit. Bauwes., Weimar 29* (1983) 75.
15. Fischer, R. and Kuzel, H.-J. *Cem. Concr. Res. 12* (1982) 517.
16. Hjorth, L. and Almeborg, J. Aalborg Portland, DK-9000 Aalborg, Denmark, personal communication (1984).
17. Kuzel, H.-J. *N. Jb. Miner. Mh.* (1966) 193.
18. Kuzel, H.-J. *N. Jb. Miner. Mh.* (1971) 477.
19. JCPDS data card No. 31-245.
20. Costa, U., Massazza, F. and Testolin, M. *Ind. Chim. Belg. 39* (1974) 587.
21. Buttler, F. G. and Taylor, H. F. W. *Cemento 75* (1978) 147.
22. Negro, A., Cussino, L. and Bacchiorini, A. *Cemento 75* (1978) 285.

Received August 29, 1985.